Available online at www.sciencedirect.com
ScienceDirect
Geochimica et Cosmochimica Acta 72 (2008) 1027–1042
Geochimica et Cosmochimica Acta
www.elsevier.com/locate/gca

Silicate and carbonate mineral weathering in soil profiles developed on Pleistocene glacial drift (Michigan, USA): Mass balances based on soil water geochemistry

Lixin Jin [a,*], Erika L. Williams [a], Kathryn J. Szramek [a,1], Lynn M. Walter [a], Stephen K. Hamilton [b]

[a] *Department of Geological Sciences, University of Michigan, Ann Arbor, MI 48104, USA*
[b] *Kellogg Biological Station and Department of Zoology, Michigan State University, Hickory Corners, MI 49060, USA*

Received 23 February 2007; accepted in revised form 7 December 2007; available online 23 December 2007

Abstract

Geochemistry of soil, soil water, and soil gas was characterized in representative soil profiles of three Michigan watersheds. Because of differences in source regions, parent materials in the Upper Peninsula of Michigan (the Tahquamenon watershed) contain only silicates, while those in the Lower Peninsula (the Cheboygan and the Huron watersheds) have significant mixtures of silicate and carbonate minerals. These differences in soil mineralogy and climate conditions permit us to examine controls on carbonate and silicate mineral weathering rates and to better define the importance of silicate versus carbonate dissolution in the early stage of soil–water cation acquisition.

Soil waters of the Tahquamenon watershed are the most dilute; solutes reflect amphibole and plagioclase dissolution along with significant contributions from atmospheric precipitation sources. Soil waters in the Cheboygan and the Huron watersheds begin their evolution as relatively dilute solutions dominated by silicate weathering in shallow carbonate-free soil horizons. Here, silicate dissolution is rapid and reaction rates dominantly are controlled by mineral abundances. In the deeper soil horizons, silicate dissolution slows down and soil–water chemistry is dominated by calcite and dolomite weathering, where solutions reach equilibrium with carbonate minerals within the soil profile. Thus, carbonate weathering intensities are dominantly controlled by annual precipitation, temperature and soil pCO_2. Results of a conceptual model support these field observations, implying that dolomite and calcite are dissolving at a similar rate, and further dissolution of more soluble dolomite after calcite equilibrium produces higher dissolved inorganic carbon concentrations and a Mg^{2+}/Ca^{2+} ratio of 0.4.

Mass balance calculations show that overall, silicate minerals and atmospheric inputs generally contribute <10% of Ca^{2+} and Mg^{2+} in natural waters. Dolomite dissolution appears to be a major process, rivaling calcite dissolution as a control on divalent cation and inorganic carbon contents of soil waters. Furthermore, the fraction of Mg^{2+} derived from silicate mineral weathering is much smaller than most of the values previously estimated from riverine chemistry.

1. INTRODUCTION

Chemical weathering has been investigated in various terrestrial environments. Carbonate minerals are more reactive and soluble than silicate minerals and thus regulate the geochemistry of surface waters (e.g., Carroll, 1970; Horton et al., 1999; White et al., 2005). Chemical weathering of silicate minerals has been proposed as a negative feedback

* Corresponding author. Present address: Center for Environmental Kinetics Analysis (CEKA), Pennsylvania State University, University Park, PA 16802, USA.
E-mail address: ljin@umich.edu (L. Jin).
[1] Present address: Department of Geology, Washington and Lee University, Lexington, VA 24450, USA.

0016-7037/$ - see front matter © 2007 Elsevier Ltd. All rights reserved.
doi:10.1016/j.gca.2007.12.007

on atmospheric CO_2 concentrations, thereby exerting control on global climate variations on geological time scales (e.g., White and Brantley, 1995; Ridgwell and Zeebe, 2005).

To better understand the fundamental controls on weathering intensity at watershed scale, our group has studied the shallow groundwater–surface water systems in recently glaciated Michigan (Szramek et al., 2007; Williams et al., 2007). Here, carbonate dissolution dominates water chemistry, and dissolved inorganic carbon (DIC) and cation fluxes are maximized by high riverine discharge and by the inverse temperature dependence of carbonate-mineral stability. Importantly, the high Mg^{2+}/Ca^{2+} mole ratios observed in surface waters and groundwaters suggest that dolomite weathering may be much more important than previously assumed when apportioning sources of riverine Mg^{2+}, Ca^{2+}, and DIC.

Previously, elemental and/or isotopic ratios have been utilized (e.g., Gaillardet et al., 1999; Quade et al., 2003; West et al., 2005) to estimate the contribution of silicate mineral weathering to stream chemistry in a watershed of mixed mineralogy (both carbonate and silicate rocks). However, Michigan streams are susceptible to anthropogenic sources (deicing salts) in densely populated, industrialized and cultivated areas (Williams et al., 2007), making the mass balance calculation very difficult.

Alternatively, we investigated soil, soil water, and soil gas geochemistry in the same Michigan watersheds where geochemistry of stream waters and groundwaters was already well established (Williams et al., 2007). In this recently glaciated mid-continental US region, a close hydrogeochemical linkage exists between soil waters, shallow groundwaters, and surface waters, which permits us to constrain the sources of riverine Mg^{2+} and Ca^{2+} and to identify the locus of mineral weathering in relatively young soil profiles. We followed the progressive evolution of soil water chemistry along hydrogeochemical flow paths and compared them among three watersheds of contrasting climate and mineralogy. Herein, we address: (1) how mineral weathering reactions are controlled by soil mineralogy and environmental factors, (2) the location in the soil profiles where most silicate and carbonate weathering occurs, and (3) the relative importance of divalent cation contributions from atmospheric precipitation, silicate mineral weathering, and carbonate mineral weathering.

2. FIELD SITE DESCRIPTION AND METHODOLOGY

During the last glacial maximum, ice sheets up to 2 km thick covered much of the North American continent. Glacier retreat left thick glacial deposits composed of diverse mineral assemblages, providing the hydrogeological setting for development of soils and regional shallow aquifers. Because glacial cycles produced extensive deposits of freshly ground mineral surfaces, weathering rates might be expected to be more rapid than those of older, more mature landscapes, analogous with the concept of weathering-limited versus transport-limited regimes of solute flux in rivers (e.g., Stallard and Edmond, 1981).

2.1. Study site characterization

The three Michigan watersheds studied, the Tahquamenon, the Cheboygan, and the Huron watersheds, are tributaries of the Great Lakes sub-basin of the St. Lawrence drainage system, and detailed descriptions of bedrock, climate and physiographic conditions in the three study watersheds have been previously presented (Fig. 1A and Table 1; Williams et al., 2007). Bedrock units of the Michigan Basin consist of crystalline Precambrian basement and an overlying succession of sedimentary rocks of Cambrian to Jurassic age (Fig. 1B; Catacosinos and Daniels, 1991). On the top of bedrocks is Quaternary glacial drift, which largely controls topographic variation (Dorr and Eschman, 1970). Because of ice sheet retreat patterns, soils in the south of Michigan are relatively older than those in the north (approximately 15,000 versus 10,500 years). The Great Lakes region receives considerable precipitation (about 80 cm/year) and it tends to be evenly distributed throughout the year. Most groundwater recharge, however, occurs in the early spring during the major snowmelt events and in the late fall. On average, about 70% of the annual rainfall is returned to the atmosphere via evapotranspiration (e.g., MacDonald et al., 1991; Rheaume, 1991).

The soil profile study sites are all located in forested areas with negligible anthropogenic influences such as clear-cutting and agriculture (Table 1). The forest composition varies (coniferous versus deciduous) as does the local topography (Fig. 2, after Williams et al., 2007). The depth to the parent drift material also varies among sites (Table 1). The study sites are denoted as follows: the Tahquamenon Falls coniferous site (TF1) and the Tahquamenon Falls hardwood site (TF2) in the Tahquamenon watershed; the Pellston Plain (PP), a mixed aspen forest in the Cheboygan watershed; and headwater forested preserve sites (HH) and the George Reserve (GR) in the Huron watershed. TF1 and TF2 are very sandy and are developed on near-shore dune deposits. Soil textures also are sandy throughout the PP area as this is an outwash plain. The Huron watershed has sites with variable lithology due to the presence of both finer-grained moraine deposits and sandy outwash areas.

Data on wet deposition chemistry are available from the National Atmospheric Deposition Program/National Trends Network (NADP/NTN) at stations near the study sites (MI-48 for the Tahquamenon, MI-09 for the Cheboygan, and MI-52 for the Huron watersheds; NADP/NTN, 2004). Volume-weighted mean concentrations of major ions from the most recent 5–10 years of monitoring are provided in Table 2. Precipitation chemistries of these three watersheds are similar, with cations dominated by Ca^{2+}, Mg^{2+}, NH_4^+, and H^+ and anions dominated by SO_4^{2-} and NO_3^-. The rainwater pH is about 4.5, reflecting sulfuric and nitric acid contributions. A pronounced air-pollution gradient is known to exist across the Great Lakes region, with deposition of SO_4^{2-} and NO_3^- increasing from north to south (MacDonald et al., 1991).

Na^+/Cl^- ratios in the wet deposition shown in Table 2 suggest that Na^+ in rain is from Cl-associated sea aerosol sources, and this is a significant contributor to the soil water Na^+. Therefore, Na^+ concentrations must be cor-

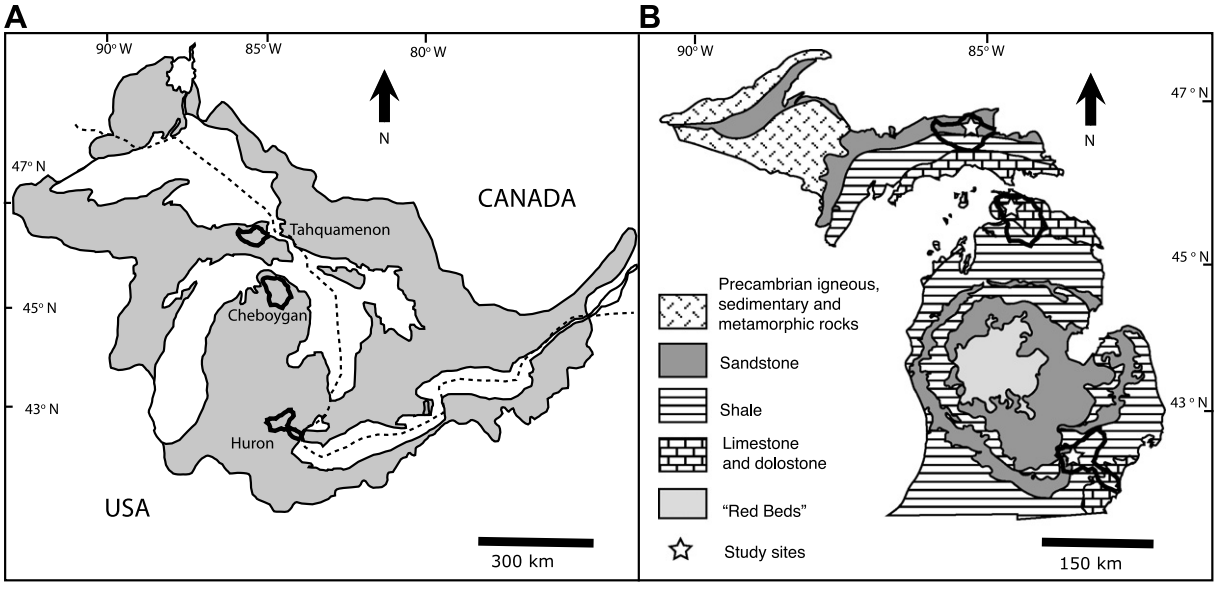

Fig. 1. The Great Lakes sub-basin of the St. Lawrence watershed (A) and Michigan bedrock geology (B, after Williams et al., 2007). Black outlines delineate the three watersheds of this study (the Tahquamenon, the Cheboygan, and the Huron watersheds from north to south). Study sites are indicated by stars. "Red Beds" includes multiple Jurassic terrestrial and marine sedimentary deposits consisting mainly of sandstone, shale and clay, with minor beds of limestone and gypsum.

Table 1
Climatic and physiographic characteristics of the three study watersheds in Michigan

Watershed	Tahquamenon	Cheboygan	Huron
Mean annual temperature (°C)	4.8	5.5	10.0
Mean annual precipitation (cm/year)	82	84	85
Drainage area (km^2)	2154	2377	2338
Bedrock geology	Sandstone, shale, limestone, dolomite	Limestone, dolomite, shale	Shale, sandstone, limestone, dolomite
Study sites	TF1 and TF2	PP	HH and GR
Glacial geology	Near-shore sandune	Outwash sand	Moraines, outwash sand and gravel
Thickness of glacial drift (m)	<15	210–270	15–30
Thickness of soilprofile (to C-horizon in m)	~1	<0.5	~1
Vegetation	TF1: pine; TF2: hardwood	Northern hardwood	Oak-hickory and beech, sugar maple

rected to estimate the amount of Na^+ derived from plagioclase dissolution (here referred to as Na^*), an approach previously applied to studies of plagioclase weathering in Ca-bearing systems (e.g., Quade et al., 2003; West et al., 2005). Soil water Na^* in our study is evaluated only for samples with Cl^- concentrations below 100 μmole/l. Uncertainty in Na^* is estimated at 17 μmole/l based on error propagation, with errors introduced mainly by variation in Na^+/Cl^- ratios of wet precipitation and by analytical uncertainty in soil water Na^+ and Cl^- determinations. For Ca^{2+} and Mg^{2+}, the maximum contribution to soil waters from wet precipitation is assumed to be three times the mean annual value due to concentration by evapotranspiration, given that 70% of precipitation is lost through evapotranspiration (Table 2).

2.2. Soil sampling and characterization

Soils were characterized at several locations at each study site. At each location, a 1.5 m-deep pit was dug, and soils were sampled at 10 cm intervals. Below 1.5 m, soils were collected by hand augering until the parent drift material (i.e., the C horizon) was reached. Soil horizons were identified in the field by soil color, texture, and an acid test for occurrence of carbonate minerals.

Soil samples for mineralogical and geochemical analyses were dried in the oven at 45 °C for 2 days, then ground to pass a 200-mesh sieve (75 μm). Selected bulk soil samples were analyzed by Scintag powder X-ray diffraction (XRD). Dominant minerals were identified and quantified using calibration curves of K-feldspar, plagioclase, and car-

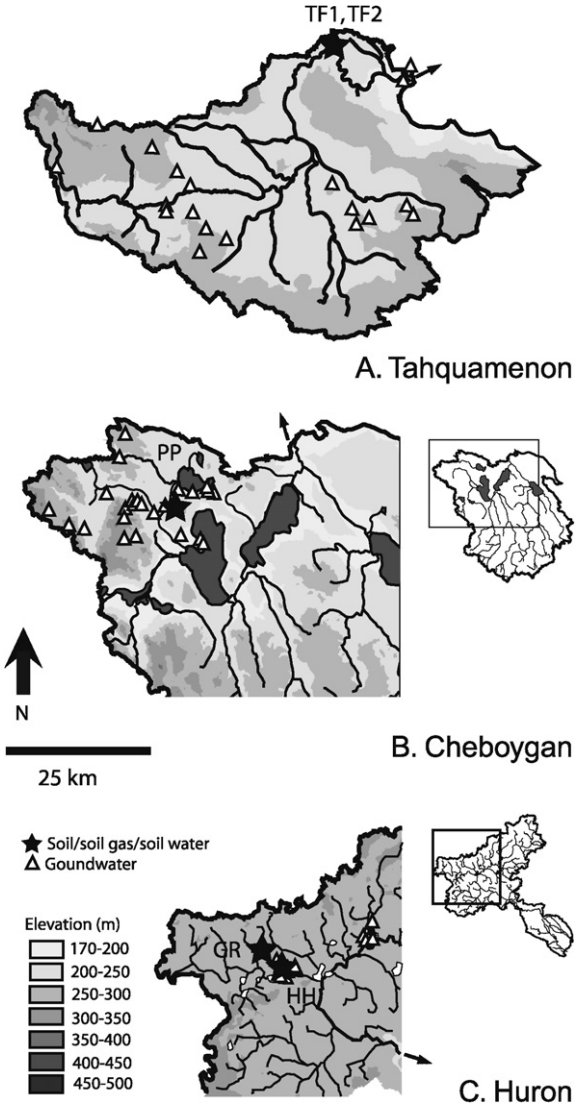

Fig. 2. Soil, soil gas and water (star) and groundwater (triangle) sampling locations are shown with topographic features for each watershed (after Williams et al., 2007), the Tahquamenon (A), the Cheboygan (B) and the Huron (C). Arrows in the maps indicate the direction of discharge from each watershed.

bonate minerals relative to quartz. Because heavy minerals (including mafic minerals and trace minerals) generally were <10% by weight, they were isolated by magnetic separator and heavy liquid methods (Lithum Heterotungstate or LST, density of 2.85) prior to XRD analysis. Thin sections were prepared for petrographic characterization from parent drift materials and heavy mineral separates at each site. Chemical compositions of plagioclase (Ca/Na ratios) were determined by electron microprobe (CAMECA SX100) at the Electron and Microbeam Analysis Laboratory (EMAL) at the University of Michigan. The clay fraction was less than 5 wt.% in all soils, and it was separated and characterized in representative soils by XRD following the methods of White and Dixon (2003) and Moore and Reynolds (1997). Solid organic carbon contents of all soil samples were determined, after acid-fuming to remove inorganic carbon, by platinum-catalyzed combustion at 900 °C with a Shimadzu TOC 5000-A total carbon analyzer with a solid sample module. Organic matter content was estimated from carbon concentrations assuming CH_2O stoichiometry.

Bulk soils were leached by aqua regia (3 HCl:1 HNO_3) at room temperature for 3 h to selectively dissolve carbonates and Al- and Fe-oxyhydroxides (Sparks, 1996). The acid leachate provides the best estimate of the total Mg and Ca carbonate content as well as the Mg/Ca ratios of the carbonate end-members. Acid leaching protocols also remove weakly held cations in the exchange pool and may dissolve a proportion of silicate minerals. Thus, cation exchange pool compositions were evaluated, focusing on Ca^{2+} and Mg^{2+} contributions. Splits of selected soil samples were analyzed for cation exchange capacity (CEC), primarily from the CEC-rich O- to B-horizons. About 2 g of dried soil were shaken in 0.1M $BaCl_2$ for 3 h, so that cations adsorbed to the exchange pool were replaced by Ba^{2+} (Gillman and Sumpter, 1986). The K^+, Al^{3+}, Ca^{2+}, Mg^{2+}, and Na^+ concentrations in the extracts were measured by a JY Ultima 2000C inductively coupled plasma optical emission spectroscopy (ICP-OES). The bulk elemental composition of soils was measured by $LiBO_2$ fusion, which dissolves both silicate and carbonate minerals including quartz. About 0.1 g samples were fused with $LiBO_2$ in platinum

Table 2
Composition of atmospheric deposition (μmole/l; NADP/NTN, 2004)

Ion	Tahquamenon	Cheboygan	Huron	Average	Max contribution to soil water[a]
Na^+	1.17	1.74	2.04	1.7	
Cl^-	1.59	2.24	2.83	2.2	
K^+	0.40	0.52	0.46	0.5	
Ca^{2+}	4.23	4.97	5.46	5.0	14.9
Mg^{2+}	0.94	1.21	1.56	1.2	3.6
SO_4^{2-}	12.28	15.01	18.64	15.0	45.0
NO_3^-	23.29	27.73	29.09	27.7	83.2
H^+	23.41	29.10	25.93	29.1	87.3
NH_4^-	19.38	20.77	24.96	20.8	62.3
pH	4.63	4.54	4.59	4.5	
Na^+/Cl^-	0.74	0.78	0.72	0.8	

[a] Max contribution assumes that evapotranspiration concentrates the soil water by three times.

crucibles at 1000 °C, then quenched and dissolved in double distilled 5% HNO_3. Cation and silica concentrations in $LiBO_2$ digests were measured using a Perkin Elmer Optima 3300DV ICP-OES.

2.3. Soil water sampling and characterization

Lysimeters (low-tension or "suction" soil water collector, 20 mm diameter, 1 μm pore size) were used to collect soil waters. Nests of lysimeters were installed at all locations. Typical sampling depths within a given nest were 15–25, 50, 75, 100, 150, 250, and 400 cm. Because some deposits were very difficult to auger, lysimeter arrays had to be placed above the parent material. This was especially problematic for the Tahquamenon watershed where a highly resistant and impermeable layer, as well as a shallow water table, prevented lysimeter placement deeper than about 2 m. After installation, the lysimeters stayed in the ground for at least a winter (more than 6 months) before sampling, a sufficient time for the lysimeters to stabilize in the field (e.g., Fölster et al., 2003). The actual depth range in the soil column sampled by the suction lysimeters is at least 6 cm above and below the mean depth of the ceramic cup due to both the cup length and the zone of influence of the capillary force. A day prior to sampling, a vacuum of −0.5 Bar was applied to draw water into the lysimeter cups.

Soil water temperature and pH were measured in the field. Great care was taken during the pH measurement to avoid the degassing of CO_2 to the atmosphere by using a sealed chamber. However, because vacuum was applied to the lysimeters, degassing could not be totally avoided (Sigfusson et al., 2006). Thus, the measured pH should be considered maximum values with an estimated uncertainty of ±0.05 pH units. Water samples were filtered through a 0.45 μm Whatman micropore filter into pre-cleaned HDPE bottles. One aliquot of each sample (50 ml) was acidified with 5–10 drops of nitric acid for cation analyses. Another filtered aliquot was left untreated for alkalinity titrations and anion analyses. All samples were maintained on ice until return to the laboratory. There, samples were stored in a dark cold room at about 4 °C until analysis.

Major cation and dissolved silica concentrations of the solutions were measured with ICP-OES, while anions were measured using a Dionex ion chromatograph (IC) in the Environmental and Analytical Geochemical Laboratory at the University of Michigan. The precision was better than ±3% for major elements and ±10% for minor elements. Total alkalinity was determined in the lab by the Gran-alk method within a day of sampling (Stumm and Morgan, 1996). The uncertainty for alkalinity titrations is less than ±2% for most samples, except for those with very low alkalinity values where uncertainty is ±0.05 meq/l. Dissolved organic carbon (DOC) was analyzed with a Shimadzu C analyzer. The charge balance for the waters analyzed was better than 5%, except for very dilute shallow O-horizon soil waters where DOC is a significant contributor to balance the charge.

2.4. Soil CO_2 sampling and analyses

Soil gas samplers were installed at sites within 2 m of lysimeter nests, at depths ranging from 20 to 200 cm. The samplers consisted of 1/8 in. ID Teflon tubing with a perforated stainless steel tip (Williams, 2005). All gas samples were collected in April/May when biological activity starts to be significant in Michigan (Ku, 2001; Jin, 2007). The soil gas samples were withdrawn in the field using 10 or 20-ml gas-tight plastic syringes after purging multiple times to clean the sampler tube. Samples were immediately transferred to pre-evacuated 4-ml glass serum vials. Soil gas pCO_2 values were measured by thermal conductivity detection in a Perkin Elmer packed column gas chromatograph (GC), calibrated with four CO_2 standards ranging from 350 to 10,000 ppmv.

2.5. Aqueous speciation calculations

Aqueous speciation and mineral saturation state of soil waters were calculated with the USGS program Solmineq.88 (Kharaka et al., 1988) using major ions, titration alkalinity, dissolved silica content, pH, and temperature as input variables. Saturation state, Ω, with respect to calcite is defined as $\Omega = [Ca^{2+}] * [CO_3^{2-}]/Ksp$, where $[Ca^{2+}]$ and $[CO_3^{2-}]$ are activities of Ca^{2+} and CO_3^{2-}, and Ksp is the solubility constant of calcite. The thermodynamic data for calcite and dolomite stability from Plummer and Busenberg (1982) and Hyeong and Capuano (2001), respectively, were used to evaluate the saturation index, $SI = \log \Omega$, of calcite and intermediate-order dolomite. Given the uncertainties in pH measurement, the degree of saturation is accurate within 0.3 SI units. Theoretical evolution of solutions produced by dissolution of calcite and dolomite in a carbon dioxide open system were also modeled using Solmineq.88 for comparison with compositions of natural soil waters, with temperature, pCO_2, and solution compositions as model input parameters.

3. RESULTS

3.1. Soil geochemistry

3.1.1. Soil acid leachates and total $LiBO_2$ digests

The elemental compositions of strong acid leachates from studied soils (Electronic Annex Table A1) show clearly that Ca and Mg contents dramatically increase below depths of about 0.8 m in the Huron watershed and 3 m in the Cheboygan watershed. This is consistent with a carbonate-leached reaction front just below the accumulation zone of Al- and Fe-oxyhydroxides in the soil B-horizon, as has been observed in Ontario glacial drift soil profiles (Reardon et al., 1979). In samples with acid soluble Mg contents above 100 mmole/kg, the Mg/Ca mole ratios were about 0.4, which corresponds to nearly equal masses of dolomite and calcite. Soil profiles from the Tahquamenon watershed do not have carbonate minerals even in the parent materials, reflecting the Canadian Precambrian Shield as the only source region. Weight percents of major cations and Si in the bulk soils were calculated from $LiBO_2$

digests and presented as oxides in Electronic Annex Table A2. As expected from bulk mineralogical analyses, silica is the most abundant oxide, followed by Al_2O_3.

3.1.2. Cation exchange capacity (CEC)

The soil cation exchange pool is assumed to be at steady state and thus not considered as a contributor to soil water solute budgets. However, contributions of the soil exchangeable pool to the cation contents determined by the strong acid leach method must be evaluated for our mass balance calculations of bulk soil mineralogy. The cation exchange pool of the soil samples is composed predominantly of Ca^{2+} and Mg^{2+}, followed by Al^{3+}, Na^+, and K^+ with total CEC ranging from 3 to 16 cmole/kg (cmole/kg = 10 mmole/kg). The Huron watershed soils have the highest CEC values, while the Cheboygan watershed soils have the lowest (Electronic Annex Table A3). The amounts of major cations leached from shallow and carbonate-free soils by strong acid treatment are close to those of CEC values, indicating that Mg, Ca, Na, and K in the acid leachate fraction originate mostly from the soil exchange pool and not from dissolution of silicate minerals. In contrast, for carbonate-bearing soil samples, the Ca, Sr, and Mg contributed by the exchangeable pool are insignificant. Thus, the Mg/Ca values of the carbonate end-member and calcite/dolomite contents indicated by the strong acid leach do not require correction for CEC contributions. Comparison of the CEC and total digest data in Electronic Annex Table A2 and Electronic Annex Table A3 shows that the contributions from the CEC are generally less than 0.01 wt.% as oxides and do not significantly affect bulk mineralogy estimates based on cation yields.

3.1.3. Soil mineralogy and carbon contents

XRD results show that quartz, K-feldspar, plagioclase, and amphibole are dominant minerals, with locally significant contributions of carbonate minerals. XRD peaks show both dolomite and calcite as pure end-members. Electron microprobe results show plagioclase has an average Na/Ca molar ratio of 4 (Ab of 0.80 ± 0.10). Combining data from the strong acid leachates, XRD, and total digests, we estimated the bulk mineralogy of these soils by mass balance (Table 3). The trace minerals identified by SEM are biotite, apatite, zircon, magnetite, ilmenite, pyrite, and sphene and the clay minerals by XRD are illite and kaolinite. As weight percentages of these minerals are insignificant, they are excluded in the following calculations.

Carbonate mineral contents are calculated from acid leachate data assuming Mg is solely from dolomite and Ca is from both calcite and dolomite. The half formula for dolomite is used for a direct comparison with calcite in terms of amount of CO_2 consumed during weathering (calcite: $CaCO_3$ and dolomite: $Ca_{0.5}Mg_{0.5}CO_3$). The carbonate mineral contents are consistent with the less precise values indicated from the XRD analyses. An amphibole composition of $Ca_2Mg_5Si_8O_{22}(OH)_2$ is assumed and it is the only Mg-bearing silicate mineral present. Thus, amphibole content can be derived from difference between Mg in the $LiBO_2$ digests and Mg in the strong acid leachates ($Mg_{silicate} = Mg_{total} - Mg_{carbonate}$). Fe is not included in the amphibole structure, and its content is calculated assuming a formula of Fe_3O_4. Plagioclase contents are derived from Na (with plagioclase composition of $Na_{0.8}Ca_{0.2}Al_{1.2}Si_{2.8}O_8$) in the total digests and K-feldspar contents are derived from K in total digests. The quartz content is calculated assuming that calcite, dolomite, K-feldspar, plagioclase, amphibole, magnetite, and quartz in total are 100%. Several errors could be introduced in these calculations. First, two separate portions of one sample are acid leached and $LiBO_2$ digested, and errors in the calculation of amphibole can result from the heterogeneity of soils. Second, magnetite is assumed to be the only Fe-bearing mineral and amphibole composition is assumed. However, these affect all sites and therefore comparison among three watersheds is still valid. Third, trace minerals and solid organic matter are not considered, which will change the quartz contents.

Carbonate minerals comprise up to 30% of soil minerals in carbonate-bearing layers, with equal amounts of dolomite and calcite present. The amounts of K-feldspar are similar among three watersheds. In contrast, the soils of the Huron watershed in the south have more Fe- and Mg-bearing minerals, more plagioclase, and less quartz than the two northern watersheds (the Tahquamenon and the Cheboygan watersheds). Plagioclase and amphibole contents and solid organic carbon concentrations are plotted against depth for all watershed soils in Fig. 3. In the Tahquamenon soil profiles, plagioclase is below detection limit in the uppermost 10 cm, likely due to plagioclase weathering (Fig. 3A). In the Huron profiles, all the soil samples have more than 10 wt.% of plagioclase and show a general trend of increasing concentration with depth. Deeper than 80 cm, the weight percent of plagioclase is influenced by the large increase in the weight fraction of carbonate minerals. Two samples from the Cheboygan profiles have 4 and 8 wt.% of plagioclase, one from the A-horizon and the other from C-horizon. Amphibole is less than 1 wt.% in Tahquamenon and Cheboygan soils but is between 1 to 5 wt.% in the Huron soils (Fig. 3B). Solid organic matter shows a general trend of decreasing with depth (Fig. 3C). In the Tahquamenon soils, solid organic carbon contents were markedly higher than in those of the other two watersheds (Fig. 3C).

3.2. Soil water and soil gas geochemistry

Soil gas pCO_2 and soil water chemistry data are reported in Electronic Annex Tables A4 and A5, respectively. Depth profiles show the vertical distribution of pH, soil gas pCO_2, DOC, total alkalinity, and calcite saturation indexes (Fig. 4). The pH is between 4 and 6 in soil waters from the Tahquamenon watershed and in the shallow soil waters from the Cheboygan watershed, similar to the pH range of precipitation. In contrast, the pH in the shallow Huron soil waters is 1 unit higher, typically between 5 and 7. Once the carbonate zone is reached, the pH quickly increases to between 7 and 8 (Fig. 4A). The soil pCO_2 values in these watersheds were 6–16 times higher than the atmospheric pCO_2 and exhibit a diffusion gradient over the uppermost 100 cm, remaining largely constant below that (see Elec-

Table 3
Soil mineralogy (in wt.%)

Site	Depth (cm)	Plagioclase	Microcline	Amphibole	Dolomite	Calcite	Fe-bearing minerals	Quartz[a]
Tahquamenon								
TF1	11	0.5	6.1	0.0			0.2	92
TF1	42	3.2	8.7	0.3			0.6	81
TF1	118	3.6	11.7	0.4			0.3	77
TF2	11	0.0	6.6	0.0			0.0	93
TF2	35	0.4	9.7	0.0			0.0	89
TF2	90	1.9	11.0	0.3			0.2	83
TF2	149	2.6	12.4	0.3			0.2	79
Cheboygan								
PP42	7	3.9	8.4	0.2			0.4	79
PP42	324	7.8	13.3	1.3	2.8	1.1	0.5	57
Huron								
GR3	10	12.3	5.2	2.2			1.7	54
GR3	23	14.1	6.4	2.6			1.9	47
GR3	36	15.3	6.1	3.4			2.2	42
GR3	48	15.2	9.6	2.7			1.5	41
GR3	64	14.0	10.9	4.6			3.7	39
GR3	68	16.6	7.4	4.0			2.9	36
GR3	96	11.9	4.8	1.3	11.8	14.2	1.9	30
GR3	140	14.9	7.0	5.0			3.1	40
GR3	180	14.0	4.7	3.2	8.9	4.3	2.4	35
GR3	235	10.6	4.5	1.7	5.2	5.8	1.1	50
GR3	280	10.3	4.4	1.9	5.1	5.8	1.0	51
HH1	80	11.3	9.3	7.4			5.9	44
HH1	100	12.3	9.8	7.0			6.5	40
HH1	148	7.3	4.8	14.4	18.4	19.6	2.9	18

[a] Weight percent of quartz is calculated assuming the total is 100%.

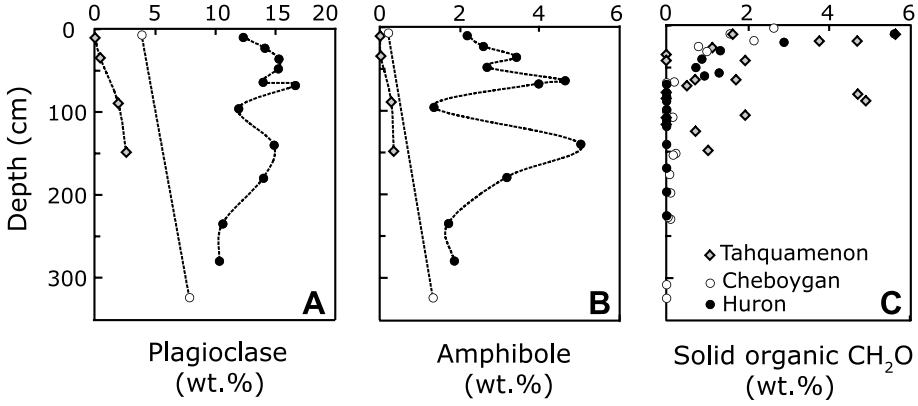

Fig. 3. Soil profiles for silicate minerals contents, plagioclase (A) and amphibole (B), and for solid organic matter contents (C).

tronic Annex Table A4 and Fig. 4B). The pCO_2 was the highest in the Huron profiles and comparable in the Cheboygan and Tahquamenon profiles. Huron soils have the longest growing season and highest mean annual temperature, so the higher pCO_2 values likely reflect higher rates of root and microbial respiration, consistent with results of prior studies (Brook et al., 1983; Savage and Davidson, 2001). The soil gas samples are representative of the start of the growing season; much higher CO_2 concentrations were observed in the summer and early fall, as CO_2 production processes are temperature dependent (Ku, 2001; Williams et al., 2003; Jin, 2007).

DOC values are highest (between 1 and 5 mmole C/l) in shallow horizons, and decrease with depth, presumably due to microbial utilization (Fig. 4C). Comparing DOC concentrations among the three watersheds, DOC was highest in Tahquamenon soils and lowest in Cheboygan and Huron soils, consistent with the differences in their solid organic matter contents. This suggests that shallow soil solution DOC concentrations were controlled by solid organic carbon contents at O-horizons. Other factors may also be important, such as mean annual temperature and the age of these solid organic materials. For example, Hongve (1999) showed that young soil organic mat-

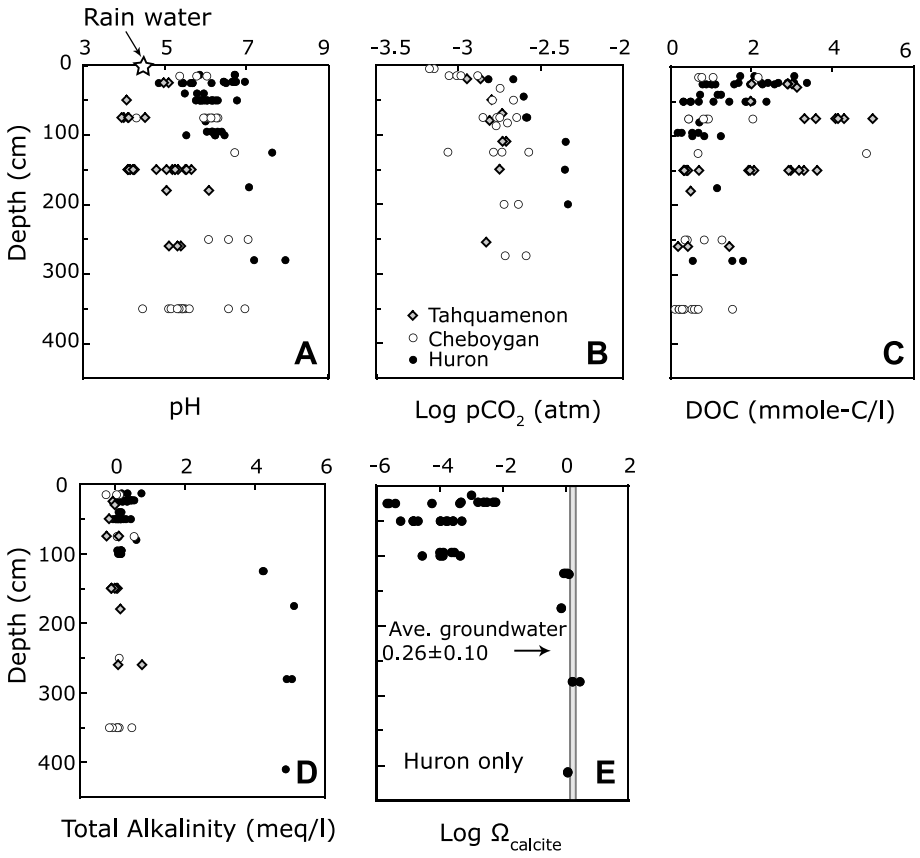

Fig. 4. Carbon transformation and transport in the soil systems and calcite saturation indexes: soil solution pH (A), soil gas logpCO_2 (B), soil water DOC (C), total alkalinity (D), and calcite saturation indexes (E) as a function of depth. The pH of the wet precipitation is indicated as a star. When the carbonate-rich layer is encountered in the shallow soil horizons, equilibrium of calcite was quickly reached and further dissolution is minimal. This is consistent with the fact that deep soil water has similar calcite saturation indexes to the Huron groundwaters (0.26 ± 0.10, shown in shadow, from Williams et al., 2007). All soil waters in the Cheboygan and Tahquamenon watersheds are extremely undersaturated with respect to carbonate minerals and these are not shown here.

ter in warm climates tends to yield higher amounts of DOC.

For shallow soil waters of the Huron watershed and all the soil waters from the Tahquamenon and Cheboygan watersheds, the alkalinity was very low (<0.6 meq/l) and even negative due to the presence of dissolved organic acids in the shallow soil zones (Cai et al., 1998). These organic acids must be neutralized before carbonate alkalinity from mineral dissolution can accumulate. In carbonate-bearing Huron soils, alkalinity reached 5 meq/l by 200 cm depth accompanied by large increases in pH (Fig. 4D). The calcite saturation indexes for the Huron watershed soil solutions are plotted against depth in Fig. 4E. In the carbonate-free Tahquamenon and Cheboygan watersheds, soil waters were hundreds of times undersaturated with respect to carbonate minerals and not plotted. As in the more northerly watershed soil waters, the shallow Huron soil waters were also highly undersaturated with respect to calcite. Only in the relatively deep carbonate-bearing soil horizons of the Huron watershed did calcite saturation states approach equilibrium values (SI: 0.06 ± 0.23). Shallow soil waters of the Huron watershed were highly undersaturated with respect to dolomite, and those deep soil waters were slightly undersaturated to close to saturated (SI: -0.25 ± 0.23). Calcite and dolomite saturation occurred at around 20 cm below the carbonate layer, implying rapid soil water equilibration with carbonate minerals. Beyond this depth, saturation indexes of carbonate minerals remain constant suggesting little additional dissolution of calcite and dolomite occurs deeper in the soil profile.

Major cation concentrations (Na^*, Ca^{2+}, and Mg^{2+}) of soil solutions are plotted with depth (Figs. 5B, 6 and 7). Na^* concentrations were about 60 μmole/l in Tahquamenon and Cheboygan soil waters while, in the Huron watershed, soil water Na^* concentrations were generally higher, reaching values of 150 μmole/l. Here, Na^* showed a sharp increase in the first 50 cm, remaining constant thereafter (Fig. 5B). In Tahquamenon and Cheboygan soils, soil water Ca^{2+} and Mg^{2+} increased very slowly with depth (Figs. 6 and 7). Soil water Ca^{2+} concentrations were less than 50 μmole/l and Mg^{2+} concentrations less than 30 μmole/l in the Tahquamenon watershed while Ca^{2+} concentrations were less than 80 μmole/l and Mg^{2+} concentrations less than 40 μmole/l in the Cheboygan watershed. Soil water Mg^{2+} and Ca^{2+} from carbonate-free soils in the Huron watershed were separated and plotted as "Huron silicate" (Figs. 6C

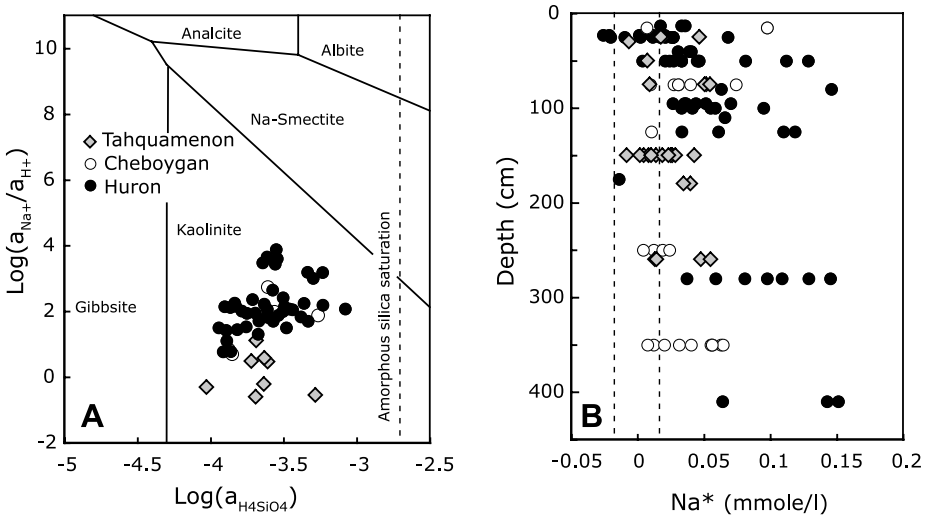

Fig. 5. The mineral stability diagram (A) indicates, that plagioclase went through incongruent dissolution and precipitated kaolinite as a secondary mineral. However, cations such as Na, Ca and Mg were released into aqueous phase stoichiometrically, therefore, acting as proxies of mineral weathering intensities. Na^* depth profiles clearly show plagioclase weathering in three watersheds (B). Na^* is defined as soil water Na concentrations after correction for atmospheric input according to Na/Cl ratios in wet precipitation. Na^* does not show a change with depth indicating majority of the plagioclase dissolution occurs at the top meter of the soil. Uncertainty of Na^* is 17 μmole/l as shown in two dashed lines.

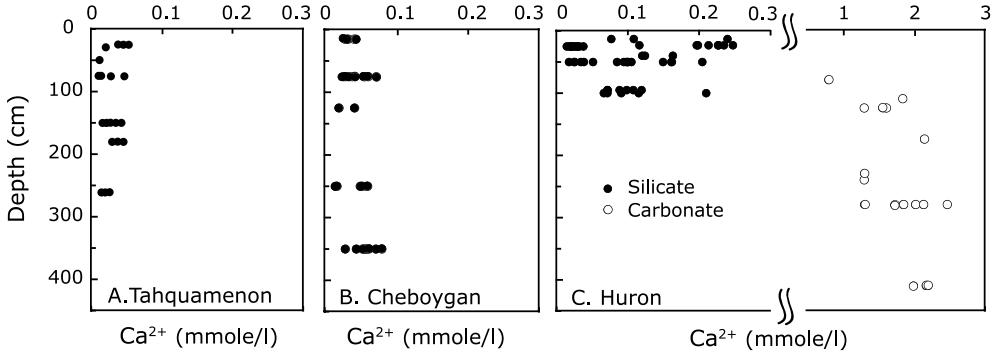

Fig. 6. Concentrations of soil-solution Ca^{2+} as a function of depth for the Tahquamenon watershed (A), the Cheboygan watershed (B) and the Huron watershed (C). Soil solutions affected by only silicate dissolution in the Huron watershed are plotted as "Huron silicate", and those by both silicate and carbonate as "Huron carbonate". The Huron depth profiles clearly show a transition from dominance by silicate weathering to dominance by carbonate weathering at around 100 cm.

and 7C). In these "Huron silicate" soil waters, Ca^{2+} reached 250 μmole/l and Mg^{2+} reached 150 μmole/l by 100 cm depth. With contributions from both silicate and carbonate mineral weathering, deep soil water Mg^{2+} was about 1 mmole/l and Ca^{2+} was about 2.5 mmole/l, exhibiting a sharp increase at the carbonate-bearing zone.

4. DISCUSSION

Because of the differences in the glacial drift sources, these contrasting soil profiles in three watersheds are primarily developed on either pure silicate or mixed silicate and carbonate parent materials (the Tahquamenon and Cheboygan watersheds versus the Huron watershed). Thick deposits of freshly eroded and reactive minerals in glacial drift provide a natural laboratory in which to determine the sequence and mass balances of carbonate versus silicate mineral weathering and to trace the hydrochemical evolution from precipitation to soil waters and then to shallow groundwaters/surface waters. Studies on geochemistry of surface waters and groundwaters in the same watersheds provide constraints on the locus and intensity of mineral weathering. Soil water elemental composition can to used to distinguish silicate-weathering contributions from those of carbonate weathering, and to estimate relative mass balances and implications for surface-water elemental fluxes and global budgets.

4.1. Chemical weathering of silicate minerals

Plagioclase and amphibole are the major silicate minerals in studied Michigan soils and they are also much more reactive and unstable than K-feldspar and quartz (e.g., Goldich, 1938; White and Brantley, 1995), both of which

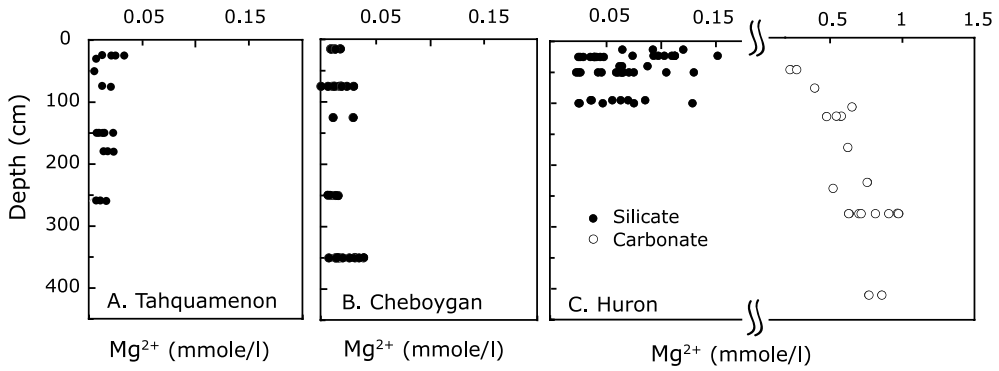

Fig. 7. Concentrations of soil-solution Mg^{2+} as a function of depth for the Tahquamenon watershed (A), the Cheboygan watershed (B), and the Huron watershed (C). Soil solutions affected by only silicate dissolution in the Huron watershed are plotted as "Huron silicate", and those by both silicate and carbonate as "Huron carbonate". The Huron depth profiles clearly show the same transition from dominance by silicate weathering to dominance by carbonate weathering at around 100 cm as seen in the Ca^{2+} profiles.

make them a major contributor of soil water Ca^{2+} and Mg^{2+} in carbonate-free profiles.

Soil water data are plotted on a Na-silicate activity diagram in Fig. 5A and all lie well within the kaolinite stability field, indicating that smectitic clay compositions are not stable. Precipitation of the secondary mineral kaolinite is consistent with the mean annual temperature and precipitation regime of the Michigan watersheds (Table 1; Velbel, 1984). Thus, plagioclase dissolution is incongruent for Al and Si, but cations such as Ca^{2+} and Na^{+} are released stoichiometrically. Because Ca^{2+} has multiple mineral sources in soil waters (plagioclase, amphibole, calcite, and dolomite), it is most reasonable to use Na^{*} as an indicator of plagioclase weathering. In addition, because Na^{+} is not significantly affected by ion exchange and biomass uptake, precipitation and mineral weathering constitute the primary sources (Stauffer and Wittchen, 1991; White and Blum, 1995).

Plagioclase contents are much lower in Cheboygan and Tahquamenon soil profiles than in those of the Huron (<4 wt.% versus >10 wt.%). These differences in abundance may in part explain the higher concentrations of soil water Na^{*} in the Huron watershed than those in the other two watersheds (e.g., Na^{*}: 150 μmole/l versus 50 μmole/l; Fig. 5B). In all three watersheds, the maximum Na^{*} concentrations are located in the most poorly buffered, carbonate-free soil horizons where DOC concentrations are also elevated. There is no evidence for an increase in Na^{*} concentration below a soil depth of about 50 cm. This is consistent with experimental studies that have shown that plagioclase hydrolysis rates increase with decreasing pH and increasing DOC concentrations (Hellmann, 1994; Oelkers et al., 1994).

At the Hubbard Brook Experiment Forest, soil solution Na^{*} was about 40 μmole/l from glacial till of granite origin (Johnson et al., 2000). Soil water Na^{+} concentrations (without correction for precipitation contribution) have been reported in streams draining granitoid-only areas (White and Blum, 1995), where stream Na^{+} concentrations range from 0 to 200 μmole/l and decrease with mean annual precipitation. Silicate minerals in the three watersheds of Michigan are of Precambrian granite origin and soil water Na^{*} concentrations in this region are as high as 150 μmole/l. Soil solution Na^{*} concentrations likely vary due to the different content of plagioclase in the soil profiles or/and different contact time of soil water and soil minerals. It has been pointed out that temperature is not well correlated with silicate weathering rates (e.g., Bluth and Kump, 1994; White and Blum, 1995). Since plagioclase contents have not been reported in previously studied areas, no direct comparison is possible. However, high soil water Na^{*} and plagioclase weathering rates in Michigan could reflect a combination of high plagioclase content in the soils, the freshly eroded mineral surfaces, and high DOC from organic matter decomposition (e.g., Blake and Walter, 1999; Anderson et al., 2000).

Mikesell et al. (2004) have shown that etching of hornblende in Michigan soil profiles increases with the soil age and decreases with increasing soil depth; etching was minimal in the deep C-horizon. This is consistent with our soil solution profiles, showing little variation in Mg^{2+} and Ca^{2+} with depth in carbonate-free soils (Figs. 6 and 7). Mg^{2+}/Ca^{2+} ratios are very high in the "Huron Silicate" soil waters, while they are low in the carbonate-free soil profiles of the Tahquamenon and Cheboygan watersheds. This is consistent with the differences in amphibole and plagioclase contents revealed by total digest analyses. The Mg^{2+}/Ca^{2+} ratios in carbonate-free Huron bulk soil digests are higher (0.5–2.5) than those of the Tahquamenon watershed soils (0–0.5) (Fig. 8A).

4.2. Equilibrium controls on carbonate mineral dissolution

The transition from silicate weathering domination to carbonate weathering domination in soil profiles occurs at around 100–120 cm in the Huron watershed (Figs. 6C and 7C). Here, soil waters also reach equilibrium with respect to calcite within the soil zones, as evidenced by similar Ca^{2+} and Mg^{2+} concentrations between deep soil waters and shallow groundwaters (Fig. 8D; Williams et al., 2007) and by similar degrees of carbonate mineral saturation (Fig. 4E). This rapid equilibration of soil waters with carbonate minerals has been observed in experimental tree growth chambers (Williams et al., 2003) and in natural shallow groundwaters (e.g., Reardon et al., 1980; Kempe et al., 1991; Ku, 2001). Thus, the amount of carbonate dissolved

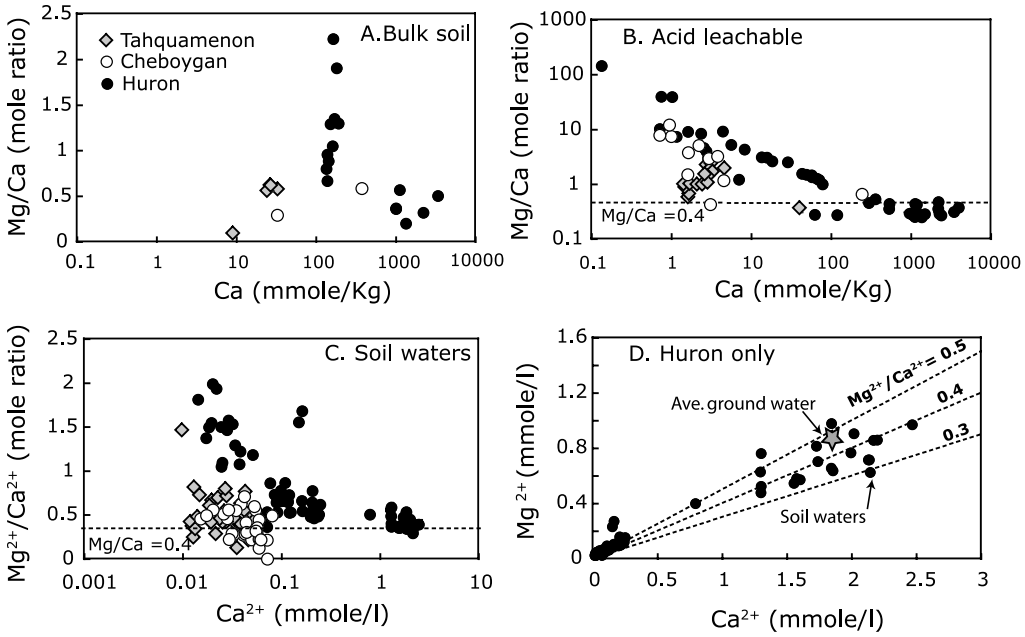

Fig. 8. Mg/Ca ratio versus Ca concentration in bulk soils by $LiBO_2$ total digests (A), in acid leachable fraction (B), and in soil waters (C). Huron soil solution Mg^{2+} and Ca^{2+} are presented in (D), where Mg^{2+}/Ca^{2+} values of 0.3, 0.4 and 0.5 are shown in reference lines. Average Huron groundwater composition is shown as a gray star in (D) after Williams et al. (2007). The Mg^{2+}/Ca^{2+} ratio is close to 0.4 (dashed line in (B) as a reference) in the acid leachable fraction indicating clearly that dolomite and calcite are both present in these soils at equal amounts and they could be up to 20 wt.% in soils. Mg^{2+}/Ca^{2+} ratios in the soil solutions and groundwaters are close to 0.4 (dashed line in (C)) when the water chemistry is controlled by carbonate dissolution (i.e., when Ca^{2+} is more than 1 mmole/l), indicating almost equal rates of dissolution for calcite and dolomite. When soil water chemistry is dominated by silicate dissolution, Mg^{2+}/Ca^{2+} ratios of the soil waters clearly reflect ratio of amphibole and plagioclase present in the soils as shown by total digests (A).

is controlled by carbonate-mineral solubility and water flux. Though the examined soil profiles in the Tahquamenon and Cheboygan watershed were carbonate-free, carbonate bedrock is present in areas of both the Tahquamenon and Cheboygan watersheds, and carbonate minerals are present in upland glacial drift deposits of the Cheboygan watershed. In the Cheboygan and Tahquamenon watersheds, carbonate weathering can take place farther along the recharge flow path, as is obvious from groundwater and surface water data which are typically more chemically evolved than soil waters (Williams et al., 2007). Previous studies have shown that pCO_2 is the major factor controlling the solubility and reactivity of carbonate minerals (e.g., Palmer and Cherry, 1984). Williams et al. (2007) show that Michigan groundwaters increase in their Ca^{2+} and Mg^{2+} concentrations from north to south in three watersheds and also appear to vary systematically in their pCO_2values (pCO_2 in log units; Tahquamenon: −2.96; Cheboygan: −2.45; and Huron: −2.13). In this study, soil gas pCO_2 is directly measured and shows a similar concentration trend (Fig. 4B). The dominant sources of CO_2 to groundwaters are rapid root and microbial respiration in shallow soil zones. If there is no additional source of CO_2, CO_2 levels in the deep ground will be lower than shallow soil zones. In the Huron watershed, carbonate dissolution permits a rapid approach to equilibrium with soil-solution cations, carbonate alkalinity, and soil gas pCO_2. This occurs within 2 m of the soil surfaces, where soil gas pCO_2 varies seasonally but is generally 10–100 times higher than atmospheric CO_2 (Fig. 4B; Ku, 2001). However, in the Cheboygan and Tahquamenon watersheds, carbonate mineral dissolution occurs farther along the flow path, where pCO_2 are very likely much lower than in the soil profiles.

Deeper soil waters in the Huron watershed have saturation states falling somewhat above calcite saturation, suggesting that further dolomite dissolution has increased the ion activity products of Ca^{2+} and HCO_3^-. The thermodynamic data for carbonate minerals shows that the equilibrium constant for dolomite exceeds that of calcite below temperatures of about 25 °C (see Langmuir, 1997), indicating that dolomite could potentially be more soluble than calcite at low mean annual temperatures. This underappreciated factor has been shown to be important in predicting the carbonate carrying capacity of surface waters and groundwaters in temperate climate zones (Szramek et al., 2007; Williams et al., 2007). Dolomite dissolution, calcite dissolution, and dolomite/calcite dissolution at equal mass amounts would produce waters with Mg^{2+}/Ca^{2+} ratios of 1, 0, and 0.33, respectively. As shown in Fig. 8C, the Mg^{2+}/Ca^{2+} ratios in these soil waters cluster at a value near 0.4. Assuming congruent dissolution without back precipitation of calcite, this value indicates that dissolution of dolomite and calcite play equal roles in regulating the soil water chemistry. Since soils contain equal amounts of dolomite and calcite (Fig. 8B), this further suggests that dolomite and calcite are dissolving at similar overall rates on a mass basis. Similar abundances of calcite and dolomite were observed in coarse-grained, carbonate bearing glacial

drift soil profiles in Trout Creek near Delhi, Ontario (Canada) (Reardon et al., 1980). There, abundance of dolomite in soils is about 10 wt.% and that of calcite is about 20 wt.% suggesting a bulk carbonate fraction Mg/Ca mole ratio of 0.2. In their soil solutions, the Mg^{2+}/Ca^{2+} ratio was 0.2, suggesting that dolomite and calcite there dissolved at proportionately the same rate.

Although Chou et al. (1989) and Morse and Arvidson (2002) report dolomite dissolution rates of several orders of magnitude lower than those of calcite, these experiments were conducted at room temperature, in low-pH solutions, and at very low degrees of saturation with respect to carbonate minerals. In field environments, natural waters typically evolve towards dolomite equilibrium because of the longer contact time between solutions and carbonate minerals. Furthermore, experimental studies of dolomite dissolution under free drift conditions (e.g., Busenberg and Plummer, 1982; Herman and White, 1985) showed that the dolomite dissolution rates depend on the source and crystallinity of the dolomite samples. Dolomite dissolution rates are higher at higher pCO_2 values and this effect is greatest at lower temperatures (Busenberg and Plummer, 1982).

Thus, as calcite and dolomite both dissolve, calcite will attain supersaturation as dolomite approaches equilibrium. However, a freshwater system often must exceed 5–10 times supersaturation before calcite precipitation could occur (Lorah and Herman, 1988) and additional mechanisms such as CO_2 degassing from surface waters and warming are required to induce precipitation (Szramek and Walter, 2004). In Michigan soils, the carbonate supersaturation occurs well below the root zone (deeper than 200 cm), and evapotranspiration will not likely lead to calcite precipitation.

4.3. Modeling dolomite versus calcite weathering

The reaction pathways and significance of dolomite dissolution in a mixed calcite/dolomite system open to CO_2 gas are illustrated here by a simple conceptual model based on the following reactions:

$$CO_2 + CaCO_3 + H_2O = Ca^{2+} + 2HCO_3^- \quad (1)$$

$$CO_2 + Ca_{0.5}Mg_{0.5}CO_3 + H_2O = 0.5Ca^{2+} + 0.5Mg^{2+} + 2HCO_3^- \quad (2)$$

In these models, the overall reaction is obtained in two reaction steps. First, dolomite and calcite dissolve at a given relative rate and the solution evolves until calcite saturation is attained. In the second step, dolomite dissolution proceeds until the solution attains saturation with respect to dolomite, producing supersaturation with respect to calcite. Calcite remains metastably supersaturated, as this supersaturaton is not enough for calcite to precipitate (suggested by field data and presented in the previous section). Model runs were conducted considering the effect of different relative rates of calcite versus dolomite dissolution (e.g., $R_{calcite}/R_{dolomite}$) using ratios of 1, 5, and 30. Carbonate system parameters and physicochemical conditions cover the range observed in the natural soil waters. A fixed pCO_2 was assumed ($\log pCO_2 = -1.5$) and runs were conducted at two temperatures (5 and 25 °C). Two solution starting points were used, one for reaction in pure water, the other in an initial solution typical of shallow soil waters influenced only by silicate mineral dissolution. The solution chemical outputs were compared for reaction step one (to calcite saturation) and for reaction step two (to dolomite saturation). Model outputs for the two starting solutions were the final total HCO_3^- concentrations, Mg^{2+}/Ca^{2+} molar ratios, and saturation indexes of calcite based on ion activities ($\Omega_{calcite}$).

Results for all the model conditions are presented in Table 4. Based on the dissolution reactions (1) and (2), HCO_3^- concentrations are controlled by mineral stability, which decreases with increasing temperatures. For example, 7.0 and 5.0 meq/l HCO_3^- are produced from calcite dissolution, at 5 and 25 °C, respectively ($\log pCO_2 = -1.5$, with or without initial Mg^{2+} and Ca^{2+}). Presence of dolomite significantly increases the HCO_3^- concentrations by up to 4.0 meq/l with the maximum increase obtained at 5 °C with $R_{calcite}/R_{dolomite}$ of 30.

The final solution Mg^{2+}/Ca^{2+} ratios obtained from the model depend on the relative reaction rates of calcite and dolomite, on the approach to calcite versus dolomite equilibrium, and to a lesser extent on the temperature. At 5 °C, near the temperature of the natural weathering environments, the final solution obtained after dolomite saturation is reached yields Mg^{2+}/Ca^{2+} ratios ranging from 0.23 for a $R_{calcite}/R_{dolomite}$ of 30 to 0.45 for $R_{calcite}/R_{dolomite}$ of 1. If the reaction is only allowed to proceed to calcite saturation, Mg^{2+}/Ca^{2+} ratios are lower, with values of 0.02 for $R_{calcite}/R_{dolomite}$ of 30 to 0.33 for $R_{calcite}/R_{dolomite}$ of 1. The continued dissolution of dolomite after calcite saturation has been reached, yielding soil waters after reaction step two which are about 2 times supersaturated with respect to calcite ($\log \Omega = 0.3$; see Table 4), which is fairly close to the values for Huron groundwaters.

Comparing these to the observed soil water Mg^{2+}/Ca^{2+} ratios in carbonate-bearing horizons of the Huron watershed (about 0.3–0.5; see Fig. 8D) suggests the natural soil water compositions can only be produced from nearly equal dissolution rates of calcite and dolomite and also by continued dissolution of more soluble dolomite. Given in the Huron watershed soils, where calcite and dolomite are present in nearly equal amounts in the deep soil horizons, the reactive surface areas of sedimentary dolomite must be much greater than those of limestone fragments to produce $R_{calcite}/R_{dolomite}$ values of 1. Possibilities include a smaller dolomite crystallite size or meta-stable dolomite structure as experimental results showed weak dependence of dolomite dissolution rates on the source rock and crystallite size (Herman and White, 1985).

4.4. Mass balance assessment of silicate versus carbonate weathering contributions

The absolute and relative contributions (in %) of wet precipitation, carbonate and silicate weathering to soil water compositions are reported in Table 5. The rainfall contribution is calculated, assuming evapotranspiration concentrates the rain chemistry by three times (Table 2).

Table 4
Mg^{2+}/Ca^{2+} ratios from modeling ($pCO_2 = 10^{-1.5}$ atm; concentrations in mmole/l)

	$R_{calcite}/R_{dolomite} = 1$		$R_{calcite}/R_{dolomite} = 5$		$R_{calcite}/R_{dolomite} = 30$		Calcite only	Dolomite only
	Step 1	Step 2	Step 1	Step 2	Step 1	Step 2		
I. Initial $Mg^{2+} = 0$ and $Ca^{2+} = 0$								
5 °C								
$\Omega_{calcite}$	1	1.94	1	2.48	1	2.73	1	1.31
HCO_3^-	7.81	10.40	7.27	10.75	7.06	10.90	7.03	9.68
Mg^{2+}/Ca^{2+}	0.33	0.45	0.09	0.28	0.02	0.23	—	1
25 °C								
$\Omega_{calcite}$	1	1.62	1	2.11	1	2.35	1	1.06
HCO_3^-	5.52	6.88	5.14	7.15	5.00	7.28	4.97	6.38
Mg^{2+}/Ca^{2+}	0.33	0.43	0.09	0.25	0.02	0.20		1
II. Initial $Mg^{2+} = 0.07$ and $Ca^{2+} = 0.10$								
5 °C								
$\Omega_{calcite}$	1	1.92	1	2.42	1	2.66	1	1.32
HCO_3^-	7.84	10.39	7.31	10.71	7.11	10.84	7.07	9.68
Mg^{2+}/Ca^{2+}	0.35	0.46	0.11	0.29	0.04	0.24	0.02	0.99
25 °C								
$\Omega_{calcite}$	1	1.59	1	2.04	1	2.25	1	1.07
HCO_3^-	5.55	6.86	5.18	7.11	5.04	7.21	5.02	6.38
Mg^{2+}/Ca^{2+}	0.35	0.44	0.12	0.27	0.04	0.22	0.03	0.98

Table 5
Atmosphere, silicate, and carbonate weathering contributions

A. Site	Ion	Soil water	Atmosphere		Plagioclase		Amphibole	
		(μmole/l)	(μmole/l)	(%)	(μmole/l)	(%)	(μmole/l)	(%)
Tahquamenon	Na*	25	—	—	25	100	—	—
	Ca	27	15	56	6	22	6	22
	Mg	13	4	31	—	—	9	69
Cheboygan	Na*	44	—	—	44	100	—	—
	Ca	46	15	33	11	24	20	43
	Mg	19	4	21	—	—	15	79
Huron (carbonate-free)	Na*	70	—	—	70	100	—	—
	Ca	100	15	15	18	18	67	67
	Mg	70	4	6	—	—	66	94
B. Site	Ion	Soil water	Atm.+Silicate		Dolomite		Calcite	
		μmole/l	μmole/l	%	μmole/l	%	μmole/l	%
Huron (carbonate bearing)	Na*	70	70	100	—	—	—	—
	Ca	2120	100	5	760	36	1260	59
	Mg	830	70	9	760	91	—	—

Cation exchangeable pool and biomass reservoirs can potentially influence soil water chemistry, but are assumed to be at steady state.

The Tahquamenon and Cheboygan soil solutions as well as the Huron soil solutions from shallow depths are dominated by silicate weathering (Figs. 6 and 7). The respective Ca^{2+} contributions from silicate weathering were 12, 31, and 85 μmole/l for Tahquamenon, Cheboygan and Huron watersheds, and Mg^{2+} contributions from silicate weathering were 9, 15, and 66 μmole/l. Studies of the chemical evolution of shallow to deep groundwaters in the sandy silicate glacial drift aquifer of north Wisconsin (Kenoyer and Bowser, 1992a,b) have initial compositions very similar to the silicate contributions for Ca^{2+} and Mg^{2+} reported here. Like Tahquamenon, the Wisconsin aquifer is composed of well-sorted glacial drift from the Canadian Shield. In their studies, evolution of shallow groundwater along a short flow path had been observed (Ca^{2+} from 25 to 125 μmole/l and Mg^{2+} from 15 to 80 μmole/l). As previously noted, wet precipitation entering deep soils after a loss of 70% by evapotranspiration can provide 15 μmole/l Ca^{2+} and 4 μmole/l Mg^{2+}. This indicates that atmospheric deposition is a significant contribution to the soil solution Ca^{2+} and Mg^{2+} budgets in the carbonate-free soils of the northern watershed (Tahquamenon: Mg^{2+} 31% and Ca^{2+} 56%; Cheboygan: Mg^{2+} 21% and Ca^{2+} 33%). In the Huron watershed, dolomite dissolution produces 1520 μmole/l total divalent cations (Mg^{2+} and Ca^{2+}), comparable to calcite dissolution (1260 μmole/l Ca^{2+}) (Table 5). Silicate dissolution and wet precipitation are relatively insignificant for

Ca^{2+} (approximate average of 100 μmole/l) and for Mg^{2+} (an average of about 70 μmole/l), and less than 10% of Mg^{2+} and Ca^{2+} is derived from these sources.

Current riverine fluxes of Mg^{2+} and Ca^{2+} to the ocean are estimated to be 137 and 550 Tg/year, respectively (Berner and Berner, 1996). Of these total divalent cation fluxes, it has been unclear exactly what proportions are derived from silicate versus carbonate mineral dissolution, and estimates based on different assumptions vary widely (e.g., Holland, 1978; Meybeck, 1987; Berner and Berner, 1996; Gaillardet et al., 1999). For example, Berner and Berner (1996) estimate that approximately 65% of the Ca^{2+} flux is derived from carbonate weathering, as opposed to silicate weathering that only accounts for 18% of the Ca^{2+} flux but accounts for 54% of the Mg^{2+}. Our results provide important support for the interpretation of groundwater and surface water chemistries from these areas reported in Williams et al. (2007). By direct measurement our results demonstrate that dolomite dissolution contributes most of the riverine Mg^{2+} and silicate mineral dissolution plays a very minor role in the mass balance. The relative weathering contributions to Ca^{2+} and Mg^{2+} fluxes we observed are fairly close to more recent estimates from global riverine flux models using bedrock type partitioning and assumed weathering products (Gaillardet et al., 1999), where 10% of the Ca^{2+} flux and 21% of the Mg^{2+} flux are derived from silicate weathering.

4.5. Significance of dolomite weathering contributions

Application of liming has been shown to efficiently neutralize soil acidity and take up atmospheric CO_2 (Oh and Raymond, 2006; Hamilton et al., 2007). Both field results and conceptual models from this study show that dissolution of dolomite in CO_2-open soil profiles enhances the carrying capacity of DIC, and calcite and dolomite together are more efficient than calcite or dolomite alone.

There is growing evidence of significant changes in the seawater Mg^{2+} and Ca^{2+} concentrations and Mg^{2+}/Ca^{2+} ratios over the Phanerozoic (e.g., Spencer and Hardie, 1990; Lowenstein et al., 2001). Major geochemical processes (exchange through mid-ocean ridge and the primary mineralogy and amount of carbonate deposition) are proposed to be responsible for the seawater changes (Von Damm, 1995; Hardie, 1996). During most of the Cenozoic, the input fluxes of HCO_3^- from the weathering of Mg-carbonates and Mg-silicates are not balanced by equivalent output fluxes of dolomite precipitation (Holland, 2005). The response of chemical weathering intensities and relative riverine inputs of Mg from carbonate versus silicate sources are important in these models. This study suggests that CO_2 drawdown by Mg-silicate may be overestimated, and thus the chemical weathering of silicate minerals would be less effective as a negative feedback of the atmospheric CO_2. To be able to quantify this on a global scale, a worldwide dolomite distribution map at the Earth's surface is required.

5. CONCLUSIONS

Although silicate dissolution in Michigan soils is incongruent, accompanied by precipitation of secondary mineral kaolinite, cations in soil waters can be characterized to place constraints on the mineral weathering intensities. Plagioclase and amphibole dissolution dominates in shallow soil profiles, and weathering rates are primarily a function of mineral abundances. Silicate dissolution is rapid within the plant root-zone, where pH is low and DOC is high and slows down into deeper soils. Further evolution of soil waters is dominated by carbonate dissolution either deeper in the soil profile (Huron) or below the water table (Tahquamenon and Cheboygan). Soil waters from deeper horizons in the Huron watershed are very similar to Huron groundwaters in chemistry, consistent with the fact that deep soil water is already saturated with respect to calcite and close to dolomite saturation. Huron soils have more carbonate dissolution, resulting from higher pCO_2 in soil zones where carbonate weathering occurs in contrast to the Cheboygan and Tahquamenon soils. In turn, the Mg^{2+}/Ca^{2+} of regional groundwaters and surface waters (Williams et al., 2007) and the Ca^{2+} and Mg^{2+} riverine discharge fluxes from these watersheds (Szramek et al., 2007) are dominantly controlled by carbonate mineral weathering. Taken together, these data demonstrate the rapid and early nature of solute acquisition and the importance of soil zone mineral dissolution as controls on the chemical composition of groundwater and ultimately river water.

In mixed mineralogy of the Huron watershed, about 5% of Ca^{2+} and 9% of Mg^{2+} are derived from silicate dissolution and wet precipitation with the rest from carbonate dissolution. Here, the Mg^{2+}/Ca^{2+} molar ratio in the soil solutions of carbonate-bearing areas indicates that equal amounts of calcite and dolomite are dissolved. Theoretical models were run in conditions similar to the field environment in the Huron watershed. A wide range of relative reaction rates between dolomite and calcite was assumed, but only when calcite and dolomite have equal dissolution rates can the soil water Mg^{2+}/Ca^{2+} ratio of 0.4 be satisfied. To explain the apparent equal dissolution rate of calcite and dolomite, dolomite must have a higher reactive surface area than calcite in the soil profiles, which could be a result of either the surface features of crystals or smaller particle sizes.

Dolomite dissolution contributes about 50% of the carbonate alkalinity and is also the dominant source of soil solution and groundwater Mg^{2+}. Further dissolution of dolomite after calcite equilibrium increases the carbon-carrying capacity of natural waters and drives the solutions to supersaturation with respect to calcite. This study emphasizes the significance of dolomite dissolution early in the weathering process in contributing to riverine fluxes and potentially influencing the seawater chemistry and global climate over geologic time.

ACKNOWLEDGMENT

We acknowledge the many assistants who worked with us in the field. Corey Lambert assisted with all aspects of the laboratory analyses and we are grateful for his enthusiastic help. We thank editor E. Oelkers and two anonymous reviewers for their comments, which greatly improved the manuscript. Financial support was provided by the National Science Foundation (EAR-0208182, EAR-0518965 and DEB-042367).

APPENDIX A. SUPPLEMENTARY DATA

Supplementary data associated with this article can be found, in the online version, at doi:10.1016/j.gca.2007.12.007.

REFERENCES

Anderson S. P., Drever J. I., Frost C. D. and Holden P. (2000) Chemical weathering in the foreland of a retreating glacier. *Geochimica et Cosmochimica Acta* **64**, 1173–1189.

Berner E. K. and Berner R. A. (1996) *Global Environment: Water, Air and Geochemical Cycles*. Prentice-Hall, Upper Saddle River, NJ, 376 p.

Blake R. E. and Walter L. M. (1999) Kinetics of feldspars and quartz dissolution at 70–80 °C and near-neutral pH: effects of organic acids and NaCl. *Geochimica et Cosmochimica Acta* **63**, 2043–2059.

Bluth G. J. S. and Kump L. R. (1994) Lithologic and climatologic controls of river chemistry. *Geochimica et Cosmochimica Acta* **58**, 2341–2359.

Brook G. B., Folkoff M. E. and Box E. O. (1983) A world model of soil carbon dioxide. *Earth Surface Processes and Landforms* **8**, 79–88.

Busenberg E. and Plummer L. N. (1982) The kinetics of dissolution of dolomite in CO_2–H_2O systems at 1.5 to 65 °C and 0 to 1 atm pCO_2. *American Journal of Science* **282**, 45–78.

Cai W. J., Wang Y. and Hodson R. T. (1998) Acid–base properties of dissolved organic matter in the estuarine waters of Georgia, USA. *Geochimica et Cosmochimica Acta* **62**, 473–483.

Carroll D. (1970) *Rock Weathering*. Plenum Press, New York, 203pp..

Catacosinos P. A. and Daniels P. A. (1991) Stratigraphy of Middle Proterozoic to Middle Ordovician formations of the Michigan Basin. *Special Paper-Geological Society of America* **256**, 53–71.

Chou L., Garrels R. M. and Wollast R. (1989) Comparative study of the kinetics and mechanisms of dissolution of carbonate minerals. *Chemical Geology* **78**, 269–282.

Dorr, Jr., J. A. and Eschman D. F. (1970) *Geology of Michigan*. University of Michigan Press, Ann Arbor, MI, 476 pp.

Fölster J., Bringmark L. and Lundin L. (2003) Temporal and spatial variations in soil water chemistry at three acid forest sites. *Water, Air, and Soil Pollution* **146**, 171–195.

Gaillardet J., Dupre B., Louvat P. and Allegre C. J. (1999) Global silicate weathering and CO_2 consumption rates deduced from the chemistry of large rivers. *Chemical Geology* **159**, 3–30.

Gillman F. P. and Sumpter E. A. (1986) Modification to compulsive exchange method for measuring exchange characteristics of soils. *Australian Journal of Soil Research* **24**, 61–66.

Goldich S. S. (1938) A study on rock weathering. *Journal of Geology* **46**, 17–58.

Hamilton S. K., Kurzman A. L., Arango C., Jin L. and Robertson G. P. (2007) Evidence for carbon sequestration by agricultural liming. *Global Biogeochemical Cycles* **21**, GB2021.

Hardie L. A. (1996) Secular variation in seawater chemistry: an explanation for the coupled secular variation in the mineralogies of marine limestones and potash evaporates over the past 600 my. *Geology* **24**, 279–283.

Hellmann R. (1994) The albite–water system: Part I: The kinetics of dissolution as a function of pH at 100, 200, and 300 °C. *Geochimica et Cosmochimica Acta* **58**, 595–611.

Herman J. S. and White W. B. (1985) Dissolution kinetics of dolomite: effects of lithology and fluid flow velocity. *Geochimica et Cosmochimica Acta* **49**, 2017–2026.

Holland H. D. (1978) *Chemistry of the Atmosphere and Oceans*. John Wiley & Sons, NY.

Holland H. D. (2005) Sea level, sediments, and the composition of seawater. *American Journal of Science*.

Hongve D. (1999) Production of dissolved organic carbon in forested catchments. *Journal of Hydrology* **224**, 91–99.

Horton T. W., Chamberlain C. P., Fantle M. and Blum J. D. (1999) Chemical weathering and lithological controls of water chemistry in a high-elevation river systems: Clark's Fork of the Yellowstone River, Wyoming and Montana. *Water Resources Research* **35**, 1643–1655.

Hyeong K. and Capuano R. M. (2001) Ca/Mg of brines in Miocene/Oligocene clastic sediments of the Texas Gulf Coast: buffering by calcite/disordered dolomite equilibria. *Geochimica et Cosmochimica Acta* **65**, 3065–3080.

Jin L. (2007) *Mg- and Ca- carbonate versus silicate dissolution rates in mid-latitude, glaciated soil profiles: implications for riverine weathering fluxes and global geochemical budgets*. Ph.D. Dissertation, University of Michigan, Ann Arbor, MI.

Johnson C. E., Driscoll C. T., Siccama T. G. and Likens G. E. (2000) Element fluxes and landscape position in a northern hardwood forest watershed ecosystem. *Ecosystems* **3**, 159–184.

Kempe S., Pettine M. and Cauwet G. (1991) Biogeochemistry of European rivers. In *Biogeochemistry of Major World Rivers* (eds. S. Kempe, E. T. Degens, J. E. Richey). John Wiley & Sons, New York, SCOPE/UNEP 42, pp. 169–211.

Kenoyer G. J. and Bowser C. J. (1992a) Groundwater chemical evolution in a sandy silicate aquifer in northern Wisconsin: 1. Patterns and rates of change. *Water Resources Research* **28**, 579–589.

Kenoyer G. J. and Bowser C. J. (1992b) Groundwater chemical evolution in a sandy silicate aquifer in northern Wisconsin: 2. Reaction modeling. *Water Resources Research* **28**, 591–600.

Kharaka Y. K., Gunter W. D., Aggarwal P. K., Perkins E. H. and DeBraal J. D. (1988) *SOLMINEQ.88: A computer program for geochemical modeling of water–rock interactions*. U.S. Geological Survey.

Ku T. C. W. (2001) *Organic carbon–mineral interactions in near surface environments: implications for the global carbon cycles*. Ph.D. Dissertation, University of Michigan, Ann Arbor, MI.

Langmuir D. (1997) *Aqueous Environmental Geochemisty*. Prentice Hall, Upper Saddle River, NY, 600 p.

Lorah M. M. and Herman J. S. (1988) The chemical evolution of a travertine-depositing stream: geochemical processes and a mass transfer reaction. *Water Resources Research* **24**, 1541–1552.

Lowenstein T. K., Timofeeff M. N., Brennan S. T., Hardie L. A. and Demicco R. V. (2001) Oscillations in Phanerozoic seawater chemistry: evidence from fluid inclusions. *Science* **294**, 1086–1088.

MacDonald N. W., Burton A. J., Jurgensen M. F., McLaughlin J. W. and Mroz G. D. (1991) Variation in forest soil properties along a Great Lakes air pollution gradient. *Soil Science Society of America Journal* **55**, 1709–1715.

Meybeck M. (1987) Global chemical weathering of surficial rocks estimated from dissolved river loads. *American Journal of Science* **287**, 401–428.

Mikesell L. R., Schaetzl R. L. and Velbel M. A. (2004) Hornblende etching and quartz/feldspar ratios as weathering and soil development indicators in some Michigan soils. *Quaternary Research* **62**, 162–171.

Moore M. D. and Reynolds C. R. (1997) *X-ray Diffraction and the Identification and Analysis of Clay Minerals*. Oxford University Press, New York.

Morse J. W. and Arvidson R. S. (2002) The dissolution kinetics of major sedimentary carbonate minerals. *Earth-Science Reviews* **58**, 51–84.

National Atmospheric Deposition Program/National Trends Network (NADP/NTN) (2004) Means of annual volume-weighted rain water composition data from Pellston (MI09), Ann Arbor (MI52) and Seney (MI48) downloaded in 2004. NADP/NTN Coordination Office, Illinois State Water Survey, 2204 Griffith Dr., Champaign, IL 61820.

Oelkers E. H., Schott J. and Devidal J. L. (1994) The effect of aluminum, pH and chemical affinity on the rates of aluminosilicate dissolution reactions. *Geochimica et Cosmochimica Acta* **58**, 2011–2024.

Oh N. H. and Raymond P. A. (2006) Contribution of agricultural liming to riverine bicarbonate export and CO_2 sequestration in the Ohio River basin. *Global Biogeochemical Cycles* **20**, GB3012.

Palmer C. D. and Cherry J. A. (1984) Geochemical evolution of groundwater in sequence of sedimentary rocks. *Journal of Hydrology* **75**, 27–65.

Plummer L. N. and Busenberg E. (1982) The solubilities of calcite, aragonite and vaterite in CO_2–H_2O solutions between 0° and 90°, and an evaluation of the aqueous model for the system $CaCO_3$–CO_2–H_2O. *Geochimica et Cosmochimica Acta* **46**, 1011–1040.

Quade J., English N. and DeCelles P. G. (2003) Silicate versus carbonate weathering in the Himalaya: a comparison of the Arun and Seti River watersheds. *Chemical Geology* **202**, 275–296.

Reardon E. J., Allison G. B. and Fritz P. (1979) Seasonal chemical and isotopic variations of soil CO_2 at Trout Creek Watershed, California. *Global Biogeochemical Cycles* **15**, 383–391.

Reardon E. J., Mozeto A. A. and Fritz P. (1980) Recharge in northern clime calcareous sandy soils: chemical and carbon-14 evolution. *Geochimica et Cosmochimica Acta* **44**, 1723–1735.

Rheaume S. J. (1991) *Hydrologic Provinces of Michigan*. U.S. Geological Survey Water-Resources Investigations Report 91-4120, 73 p.

Ridgwell A. R. and Zeebe R. E. (2005) The role of the global carbonate cycle in the regulation and evolution of the Earth system. *Earth and Planetary Science Letters* **234**, 299–315.

Savage K. E. and Davidson E. A. (2001) Interannual variation of soil respiration in two New England forests. *Global Biogeochemical Cycles* **15**, 337–350.

Sigfusson B., Paton G. I. and Gislason S. R. (2006) The impact of sampling techniques on soil pore water carbon measurement of an Icelandic Histic Andosol. *The Science of the Total Environment* **369**, 203–219.

Sparks D. L. (1996) Methods of soil analysis: Part 3. Chemical methods and processes. Soil Sci. Soc. Am. Book Series 5, SSSA, Madison, WI.

Spencer R. J. and Hardie L. A. (1990) Control of seawater composition by mixing of river waters and mid-ocean ridge hydrothermal brines. In *Fluid–Mineral Interactions: A Tribute to H. P. Eugster* (eds. R. J. Spencer and I. M. Chou). Geochemical Society Special Publication 19, pp. 409–419.

Stallard R. F. and Edmond J. M. (1981) Geochemistry of the Amazon 1: precipitation chemistry and the marine contribution to the dissolved load at the time of peak discharge. *Journal of Geophysical Research* **86**, 9844–9858.

Stauffer R. E. and Wittchen B. D. (1991) Effect of silicate weathering on water chemistry in forested, upland, felsic terrane of the USA. *Geochimica et Cosmoica Acta* **55**, 3253–3271.

Stumm W. and Morgan J. J. (1996) *Aquatic Chemistry*, third ed. Wiley-Interscience, New York.

Szramek K. and Walter L. M. (2004) Impact of carbonate precipitation on riverine inorganic carbon mass transport from a Mid-continent, forested watershed. *Aquatic Geochemistry* **10**, 99–137.

Szramek K., McIntosh J. C., Williams E. L., Kanduc T., Ogrinc N. and Walter L. M. (2007) Relative weathering intensities of calcite vs. dolomite in carbonate-bearing temperate zone watersheds: carbonate geochemistry and fluxes from catchments within the St. Lawrence and Danube River Basin. *Geochem. Geophys. Geosyst.* **8**, Q04002. doi:10.1029/2006GC001137.

Velbel M. A. (1984) *Mineral transformations during rock weathering and geochemical mass-balances in forested watersheds of the southern Appalachians*. Ph.D. Dissertation, Yale University, New Haven, CT.

Von Damm K. L. (1995) *Controls on the chemistry and temporal variability of seafloor hydrothermal fluids, in seafloor hydrothermal systems: physical, chemical biological, and geological interactions*. American Geophysical Union, Geophysical Monograph 91, pp. 222–247.

West A. J., Galy A. and Bickle M. (2005) Tectonic and climatic controls on silicate weathering. *Earth and Planetary Science Letters* **235**, 211–228.

White A. F. and Blum A. E. (1995) Effects of climate on chemical weathering rates in watersheds. *Geochimica et Cosmochimica Acta* **59**, 1729–1747.

White A. F. and Brantley S. L. (1995) Chemical weathering rates of silicate minerals: an overview. In *Chemical Weathering Rates of Silicate Minerals, vol. 31, Reviews in Mineralogy and Geochemistry* (ed. A. F. White and S. L. Brantley). Mineralogical Society of America, pp. 1–22.

White A. F., Schulz M. S., Lowenstern J. B., Vivit D. V. and Bullen T. D. (2005) The ubiquitous nature of accessory calcite in granitoid rocks: implications for weathering, solute evolution, and petrogenesis. *Geochimica et Cosmochimica Acta* **69**, 1455–1471.

White G. N. and Dixon J. B. (2003) *Soil Mineralogy Laboratory Manual*. Published by the author, Department of Soil and Crop Sciences, Texas A& M University, College Station, TX 77843-2474.

Williams E. L. (2005) *Carbon cycling and mineral weathering in temperate forested watersheds: an integrated study of solution and soil chemistries*. Ph.D. Thesis, University of Michigan, Ann Arbor.

Williams E. L., Walter L. M., Ku T. C. W., Kling G. W. and Zak D. R. (2003) Effects of CO_2 and nutrient availability on mineral weathering in controlled tree growth experiments. *Global Biogeochemical Cycles* **17**, 1041–1052.

Williams E. L., Szramek K., Jin L., Ku T. C. W. and Walter L. M. (2007) The carbonate system geochemistry of shallow groundwater/surface water systems in temperate glaciated watersheds (Michigan, USA): significance of open system dolomite weathering. *Geological Society of American Bulletin* **119**, 515–528.

Associate editor: Eric H. Oelkers